Desalination and Water Treatment
www.deswater.com

doi: 10.5004/dwt.2020.25719

192 (2020) 226–233
July

Optimized fabrication of chitosan-hydroxy apatite (HAp/CS) nano hybrid for removal of nitrite from water samples

Mohaddeseh Habibi, Amir Bagheri Garmarudi, Mohammadreza Khanmohammadi Khorrami*, Shima Zandbaaf, Donya Arjmandi

Chemistry Department, Faculty of Science, Imam Khomeini International University, Qazvin, Iran, emails: m.khanmohammadi@sci.ikiu.ac.ir/ mrkhanmohammadi@gmail.com (M.K. Khorrami), habibi.mohadese431@gmail.com (M. Habibi), bagheri@sci.ikiu.ac.ir (A.B. Garmarudi), shima_zandbaf@yahoo.com (S. Zandbaaf), donya.arjmandi@gmail.com (D. Arjmandi)

Received 9 January 2018; Accepted 16 February 2020

ABSTRACT

Chitosan/hydroxyapatite (HAp/CS) nanohybrid has been fabricated in an optimized synthesis condition to be employed for the removal of nitrite from water samples. The method was optimized using the design of experiments developing a three-factor, central composite design model. Particle size of the optimum nanohybrid was 17.1 nm. HAp/CS as an adsorbent hybrid was also characterized by X-ray diffraction and Fourier transform infrared spectroscopy to specify its morphology, functionality, and structure. In order to remove nitrite ions by the nanohybrid, cross-linked chitosan-apatite nanohybrid was prepared and the process was monitored by UV-visible (UV-Vis) spectrophotometry. The UV-Vis spectrum of cross-linked chitosan-apatite nanohybrid suspension was recorded every 5 min to obtain and evaluate the analyte concentration. Also, the evolution of the adsorption process was investigated by multivariate curve resolution-alternating least squares method.

Keywords: Chitosan/hydroxyapatite (HAp/CS); Nano hybrid; Optimization; MCR-ALS; Nitrite; CCD

1. Introduction

Environmental efforts have been focused to provide clean water as an important goal in life aspects. Removal of pollutants from water has remained a major global challenge [1–3]. As an example, high nitrite levels in water are known as a pollution which can cause methemoglobinemia or blue baby syndrome [4]. Nitrate (NO_3^-) is an anion which its presence in water resources and groundwater aquifers has created serious problems all around the world. One of the most important factors which many increase the level of nitrate concentration is the overuses of fertilizers and industrial productions. This phenomenon can cause a serious health risk for human and animals [5–7]. Currently, in order to decline the concentration of nitrate in potable water and control it, different methods such as ion exchange (IX), reverse osmosis (RO), electro dialysis (ED), and biological denitrification (BD) have set in many countries. Although these methods are considered as useful technologies to eliminate nitrate in the water which offer operational information gained from valuable industry experiences, these also suffer from drawbacks as well. The most common disadvantages of these techniques are high costs, poor performance in solving the problems relevant to the excess nitrate in the environment and waste water production because of highly brine content. In recent years, adsorption by natural materials has shown to be one of the most efficient and low cost methods for ion removed from aqueous solution. So far, various types of natural adsorbents, such

* Corresponding author.

as activated carbons, chelating materials, biosorbents, and chitosan (CS)/natural zeolites have been employed for the adsorption of ions from aqueous solutions [5,7–15].

Chitosan [β-(1–4)-linked-2-amino-2-deoxy-D-glucose] is a type of natural polyamino-saccharide, known as the second most abundant natural polysaccharide after cellulose [16,17]. Its noticeable properties, for example, adsorption capacity, hydrophobic nature, biocompatibility, biodegradation rate, and non-toxicity, widens its applications. However, it has some physical and chemical deficiencies which can be improved by several strategies such as hybridation, grafting, and cross linking. Among different deficiency improvement routes, hybridation is known to be efficient in enhancement of selectivity, regeneration, surface area, mechanical strength, and surface behavior of chemicals [18]. Chitosan based hybrids have been fabricated to adsorb pollutants from water samples [19,20]. Calcium hydroxyapatite (HAp) is an inorganic biomaterial, which shows good ionic exchange ability for both cation and anion structures, due to its unique channel as a high efficient adsorbent to remove ions from water samples [21–23]. Hydroxyapatite/chitosan (HAp-CS) nano hybrid has been employed in biomedical applications and some environmental pollutant removal process such as adsorption of dyes and heavy metals have been studied [24,25]. An important part of an experimental investigation is to optimize the procedure condition [26,27]. In case of nanohybrid fabrication, it is necessary to optimize the size and morphology of the obtained hybrid, considering the experimental parameters which may influence the output. Design of experiments (DOE) is a well-known approach for this aim. In this paper, HAp-CS composites were prepared with co-precipitation method, being optimized to achieve the minimum size of HAp-CS nano hybrid. The HAp-CS nano hybrid obtained by optimal condition was cross linked by N,N-methylenebisacrylamide, and then being used to remove of nitrite contaminant from water samples. Hence, the present study is aimed to extend the application of HAp-CCS nano hybrid for removal nitrite ions from water samples. The removal process was also monitored by UV-visible (UV-Vis) spectroscopy. Then, obtained data were processed by multivariate curve resolution-alternating least squares is (MCR-ALS) method.

2. Experimental

2.1. Materials and apparatus

Chitosan from Suvchem (India), calcium nitrate ($Ca(NO_3)_2$) and sodium nitrite ($NaNO_2$) from Sigma Aldrich, ammonium dihydrogen phosphate and ammonia from Merck (Germany), all were of analytical grade.

The UV-Vis spectrophotometer was from Camspec Co. The particle size of nano hybrids was determined by dynamic light scattering (DLS) Courduan technologies **VASCO,** laser diode 658 nm/15 mW, and morphology of synthesized nano hybrids was determined by a field emission scanning electron microscope (FESEM) (30 kV, model 4160, Hitachi, Japan). In order to digitalize the IR spectral data, WINFIRST software V.3.57 was used. Process optimization was conducted by MINITAB software V.7. MCR-ALS GUI user-friendly graphical interface was run in Matlab 2014 [28].

2.2. Synthesis of HAp-CS nano hybrid

HAp-CS hybrid fabricated with different CS contents (according to DOE model). Chitosan was firstly dissolved in glacial acetic acid (2%), being stirred continuously for 3 h to acquire a homogenous gel. CS gel was then mixed with $Ca(NO_3)_2{\cdot}4H_2O$ solution with a stoichiometric ratio of Ca/P = 1.67. In the next step $(NH_4)_2HPO_4$ solution was added to CS–Ca $(NO_3)_2$ solution at the rate of 5 mL/min in the volume ratio of 3:2. The pH of the reaction was maintained above 10 using ammonia solution during the entire addition process and continuous stirring for 4 h. The obtained suspension was filtered with vacuum pump and the precipitate was rinsed with deionized water until the pH of filtrate was close to 7. Then the HAp-CS hybrid was further rinsed with ethanol, being dried at designed temperature. Chemical cross-linking of the HAp-CS nano hybrid was performed to improve pore size, hydrophilicity, and improve adsorption capacity by interpolation of new functional groups on HAp-CS nano hybrid. Thus HAp-CS was dispersed in deionized water, being stirred for 1 h at room temperature. Then C_3H_5NO (1.0 g), $C_7H_{10}N_2O_2$ (MBA) (0.1 g), and $(NH_4)_2S_2O_3$ (0.1 g) were added to the suspension, being further stirred for 2 h at 80°C. The obtained suspension was centrifuged and rinsed with ethanol deionized water. The precipitate was dried at 40°C in vacuum oven for 12 h.

2.3. Experimental design and statistic

A central composite design (CCD) with response surface methodology (RSM) was applied for optimization. The RSM model was equipped with statistical tools to determine the significance of a factor over a response. The RSM focused on the construction of geometrical approaches which can predict the behavior of the factors in the evaluation area. On the other hand, RSM enables the independent evaluation of each factor and their interaction within the proposed model. In order to evaluate the influence of operating parameters on the particle size (response, *Y*), studied factors were CS: HAp (30%, 50%, and 70% w/w), pH (10–12) and drying temperature (80°C–150°C). A total number of 20 runs were created by this design for the three studied factors of the CCD model (Table 1). Size of the fabricated nano hybrids was determined by DLS, and their morphology was studied by FESEM.

2.4. Nitrite removal

2.4.1. Determination of the adsorption capacity

Sodium nitrite ($NaNO_2$) was dissolved in deionized water to prepare stock solution. Then test solution were prepared in the concentrations ranges of 50–100 mg L^{-1}. In the next step 0.05 g HAp-CCS nano hybrid was added to nitrite solution in a conical flask being horizontally shaked at shaking frequency of 120 rpm at room temperature (25°C). The solution was filtered and the remaining nitrite concentrations was determined using UV/Vis spectrophotometer at 400–600 nm, according to the colorimetric assay based on the Greiss reaction method [29]. The same procedure was applied for determination of nitrite ions adsorbed per gram

of sorbent (simply the unit will be noted as mg/g), being calculated using the general Eq. (1) [30]:

$$q_e = \frac{(C_0 - C_e)V}{M} \quad (1)$$

Table 1
Central composite design (CCD) experimental in different runs and the responses obtained

Run	X_1	X_2	X_3	Y
1	0	0	1.68	31.3
2	0	0	0	23.4
3	1	1	1	15.7
4	–1	–1	1	35.6
5	0	1.68	0	15.6
6	1	–1	–1	42.3
7	0	0	–1.68	36.2
8	–1.68	0	0	21.1
9	1.68	0	0	56.7
10	0	1	–1	24.3
11	0	1	1	27.3
12	0	–1.68	0	32.2
13	0	–1	–1	31.3
14	1	–1	1	45.0
15	1	1	–1	39.1
16	0	0	0	23.4
17	0	0	0	27.5
18	0	0	0	23.5
19	0	0	0	27.3
20	–1	–1	–1	31.3

X_1, X_2, and X_3 are studied variables and Y is nanohybrid's size (nm).

where q_e is the adsorption capacity (mg/g), C_0 and C_e are the initial and equilibrium concentrations of nitrite ions in the liquid phase (mg/L), respectively. V is the volume of the solution (mL) and M is the amount of HAp-CCS nano hybrid (g).

2.4.2. Effect of contact time

In order to disclose contact time, 0.05 g of the (HAp-CCS) nano sorbent was added to 50 mL of nitrite solution (100 mg/L) in a flask and the contents were shaken at room temperature at 200 rpm for a time period of 5–60 min. Then the contents were filtered, being analyzed to determine the sorption capacity.

3. Results and discussion

3.1. Characterization of the sorbents

The X-ray diffraction (XRD) analyses were performed on HAp powder, CS, and CS-HAp hybrid samples using a diffractometer. The XRD was further employed to reveal the crystallographic evaluation of the prepared sorbents. As observed in Fig. 1, Crystalline signal of HAp at 2θ = 26.0°, 31.9°, 33.1°, 34.2°, and 39.9° would appear in HAp-CS composites. This indicated that there was no significant change in the crystalline structure after the composite formation [31].

The particle size and morphology of fabricated HAp, and HAp-CS hybrid were studied using FESEM. Typical SEM image of both samples, is shown in Fig. 2. Nano hybrids were all spherical with appropriate morphology and nano hybrids distribution is similar.

Fourier transform infrared (FTIR) spectra of chitosan, Hap, and HAp-CS hybrid in the 400–4,000 cm^{-1} spectral region were recorded and have been presented in Fig. 3. The FTIR spectrum of HAp shows stretching vibrations at 632 and 3,140 cm^{-1} due to hydroxyl groups. The bands at 560–610 cm^{-1} and 1,000–1,100 cm^{-1} correspond to

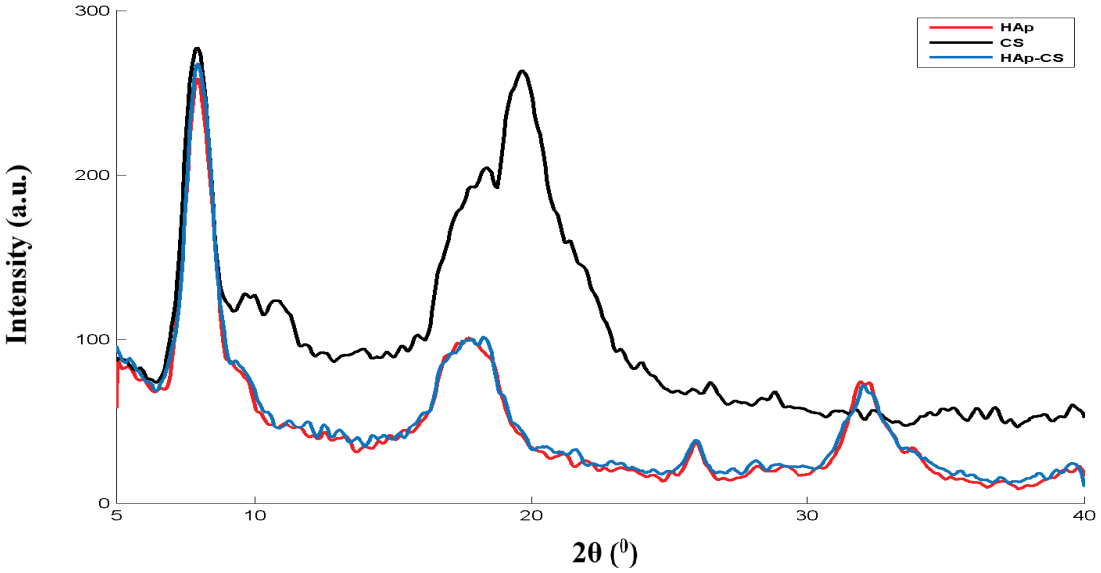

Fig. 1. XRD pattern of CS, HAp, and HAp-CS.

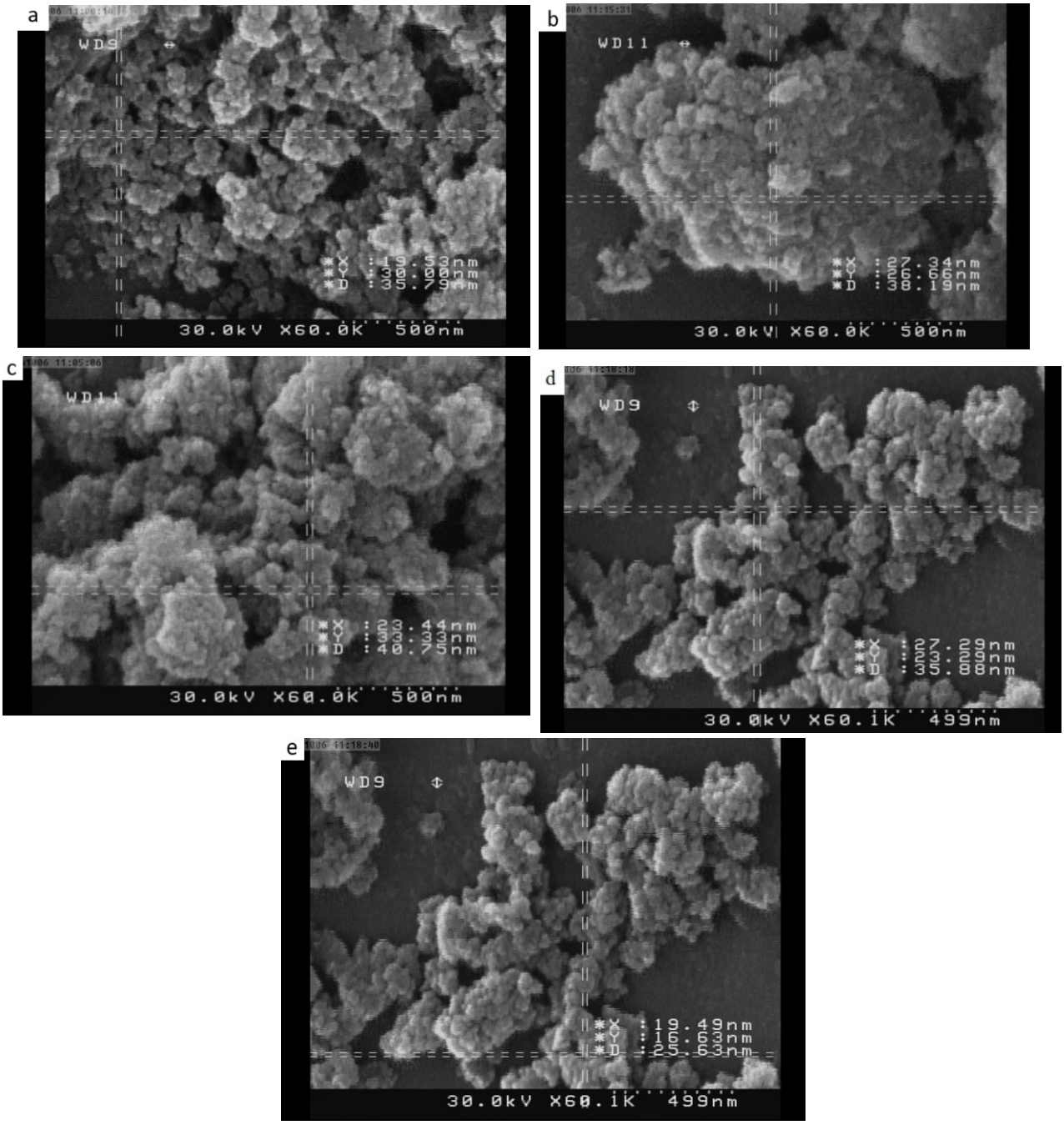

Fig. 2. FESEM images of (a) CS-HAp 30%, (b) CS-HAp 70%, (c) CS-HAp 50%, (d) apatite, and (e) optimized HAp-CS nanohybrid.

PO_4^{-3} stretching vibrations [32,33]. Fig. 3b shows a band at 1,636 cm^{-1} due to C=O group of chitosan in the hybrid. In Fig. 3b, C the –NH group of chitosan makes spectral features at 1,634 and 3,140 cm^{-1}. The bands at 2,850; 1,460; 1,383 $cm^{-1}$are attributed to the vibration of –CH group of chitosan. The vibration bands of C–O group are overlapped with phosphate bands at 1,150–1,040 cm^{-1}. Thus, by incorporation of CS into HAp, the two specific bands of amino groups (3,370 and 1,599 cm^{-1}) would shift to higher wavenumbers which indicate feasible interactions between CS and HAp. According to the structures of CS and HAp, these interactions may contain hydrogen bonding between OH of HAp and NH_2 of CS as well as chelating between Ca^{2+} and NH_2.

3.2. Effect of variables on the size of HAp-CS nano hybrid

In order to evaluate the experimental design model, particle size was determined for different combinations of the parameters to study the combined effects of these factors, and obtained result from model, provided the effect of variables in response as Eq. (2).

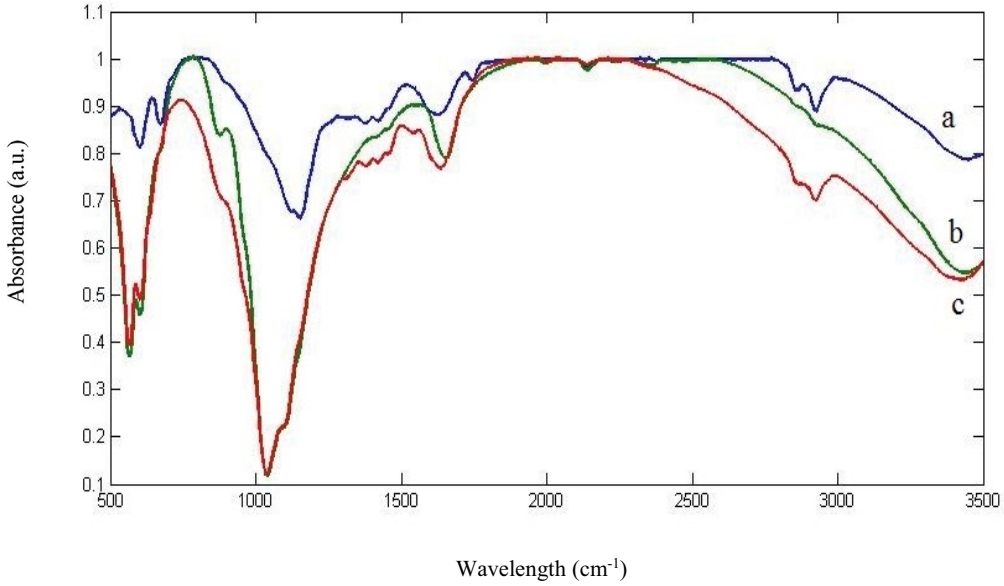

Fig. 3. FTIR spectra of (a) chitosan, (b) apatite, and (c) CS/HAp in the 400–4,000 cm^{-1} spectral region.

$$Y = b_0 + b_1A + b_2B + b_3C + b_1b_2AB + b_1b_3AC + b_2b_3BC + b_{11}A^2 + b_{22}B^2 + b_{33}C^2 \quad (2)$$

In Eq. (2), Y, A, B, and C, are the response (nano hybrid size), the HAp-CS ratio, pH of reaction, and dry temperature, respectively. Also, b_0 is constant regression coefficient, and b_1–b_3 are the coefficients of variables A, B, and C. Linear, quadratic, and interactive terms conformity are evaluated with result of the test. The linear model was found to be the most suitable model. Analysis of variance (ANOVA) can be used to realize the effect of variables. In this analysis, p-value can be used the survey the importance of coefficients. p-value less than 0.05 indicate that model terms are significant with in selected conditions. The tests for significance of the regression model were evaluated and the results of ANOVA have been presented a table in supplementary documents. In this case A, B, and AB are significant model terms. Thus, HAp-CS ratio and pH are more influent upon the response between studied parameters that can be synergistic effect and antagonistic effect, respectively. In case of lack of fit, p-value was greater than 0.05, and thus it is not significant. Relationships between variables and responses are presented by Eq. (3):

$$Y = 27.28 + 12.15A - 7.61B + 14.33AB \quad (3)$$

A positive sign in the equation represents a synergistic effect of the variables, while a negative sign indicates an antagonistic effect of the variables. The correlation measure for testing fitting quality of the regression equation was adjusted correlation coefficient (R^2_{adj}). The value of adjustable R^2 was calculated to be 73.25% for Eq. (3). The R^2 value provides a measure of variation in the observed response values and can be explained by the experimental factors and their interactions. When expressed as a percentage, R^2 is interpreted as the percent variability in the response explained by the statistical model. The sample variation of 73.25% for Eq. (3) was degree of correlation between the observed and predicted values.

The effect of HAp-CS ratio (A) and pH of reaction (B) on the nano hybrid size (Y) is shown in Fig. 4a. The nano hybrid size is decreased by increasing pH and decreasing ratio of HAp-CS. This could be possibly attributed to degree of crystallization in apatite by pH increment, and while it is reduced the size of nano hybrid is more fine.

Fig. 4b shows the residual plots for nanohybrid size in this model. The regression analysis to error variance should be around zero, otherwise model is unreliable. In fitted value plot, residual value explains if the model is suitable or not. It also provides fitted normal distribution and the response randomly and symmetric scatter in the residual plots.

During above-mentioned, steps the synthesis methods were optimized. In accordance with CCD experimental design, optimum HAp-CS ratio, pH 36%, and 12.7, being used for the fabrication process. The optimized response was estimated to be 17 nm. HAp-CS nano hybrid was prepared based on the optimized method, being modified by MBA cross-linking and employed in nitrite removal from water samples. Chitsoan was dissolved in acetic acid and ionized amine group, chitosan shows great tendency to react with PO_4^{3-} based ions (consisting of PO_4^{3-}, HPO_4^{2-}, and $H_2PO_4^-$), in the next step negatively charged PO_4^{3-} sites would incorporate with positive charged calcium ions and incept nucleation process of nano-sized HAp particles on CS and then cross linking with MBA would occur according to section 2.3.1 (Fig. 5).

3.3. Effect of contact time

The isotherm for adsorption of nitrite by optimized HAp-Cross linked CS hybrid is displayed in Fig. 6. The nitrite ions removal was very fast at the beginning (within 30 min), being continued by a slower kinetics until equilibrium.

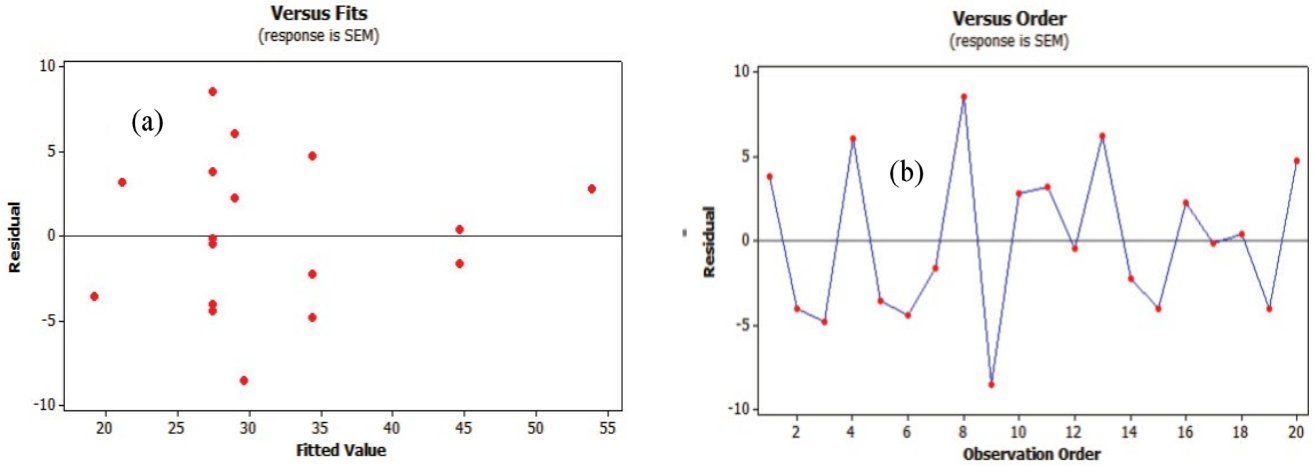

Fig. 4. Residual plots for *Y* according to the model Eq. (3).

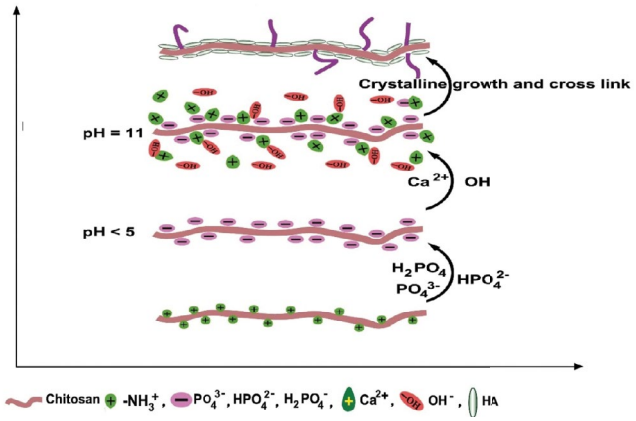

Fig. 5. Proposed mechanism for nHA crystalline formation.

Generally, it was noticed that a contact time of 60 min is sufficient to ensure the capacity saturation for the nitrite ions sorption.

3.4. UV-Vis spectroscopy multivariate curve resolution

In order to perform nitrite removal by the nano hybrid, cross linked chitosan-apatite nanohybrid was examined in 60 min according to previously mentioned procedure and process was monitored by UV-Vis spectrophotometry in 400–600 nm spectral region. The UV-Vis spectrum of cross linked chitosan-apatite nano hybrid solution was recorded every 5 min to obtain and evaluate the equilibrium concentration. The results from UV-Vis spectra demonstrate that the λ_{max} is 510 nm. The obtained spectra showed a gradual reduction in concentration of nitrite till 50 min and stable concentration after wards. MCR-ALS chemometric method was employed to the spectral process data. It is assumed that there is a bilinear relationship between data. Consequently, data matrix is decomposed as follows:

$$D = CS^T + E \quad (4)$$

where D, C, S^T, and E are data matrix, concentration profile, spectral profile, and error matrix, respectively. Before decomposition of data matrix, it is essential to determine the number of active components in the evaluated system and this task is performed by principal component analysis (PCA). Then, decomposition is performed by an initial estimation of one of the concentrations or spectral profiles, utilizing a curve resolution method such as evolving factor analysis (EFA). Estimated profile is used in the above equation to get other profiles and in next stage the profile resulted in this stage is applied to calculate the profile realized in previous stage. This process continues to reach convergence and profiles with minimum error is calculated. Least squares (LS) calculation is error criteria. During decomposition of data matrix to concentration and spectral profiles, ambiguities are one of the main problems that are encountered. In order to solve ambiguity problem, application of some constraints such as no negativity which assumes that there are not negative values in concentration and spectral profile and unimodalty which assumes one maximum in profiles is helpful [28,34,35].

Spectra of nitrite solution were recorded during adsorption process. These spectra were applied as a data matrix while its rows were the time and its columns were wavelengths, to investigate concentration profile of nitrite. PCA revealed that there is one active component in system. After performing of EFA, resulted concentration profile was used as initial estimation. The resolved concentration profile obtained from MCR-ALS has been shown in Fig. 7. Resolved profiles affirm the results of UV-Vis spectra. It means that adsorption of nitrite on adsorbent unit 20 min would be gradual and after that unit 50 min is would be faster.

3.5. Desorption study

One of the important parameters featuring powerful sorbents is its regeneration tendency. The anions adsorbed on this were replaced by OH^-. The adsorbents regained their original form after treating with excess amount of deionized water.

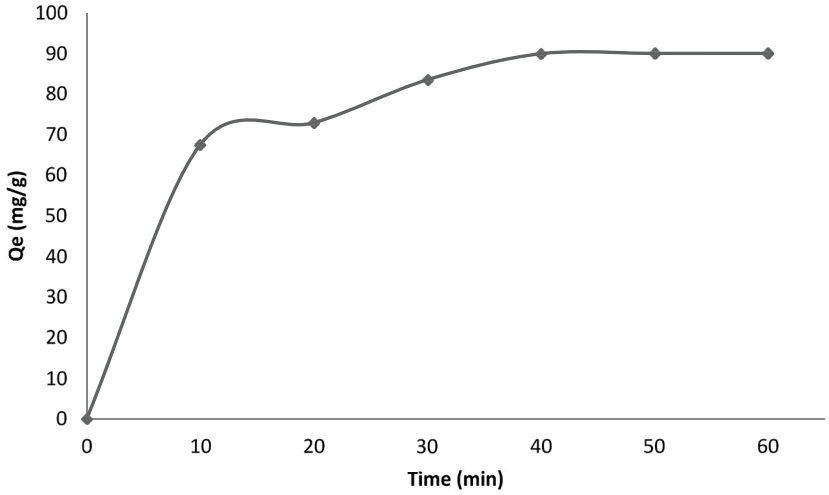

Fig. 6. Effect of contact time on the sorption capacity of nitrite ions on to HAp-CS nanohybrid.

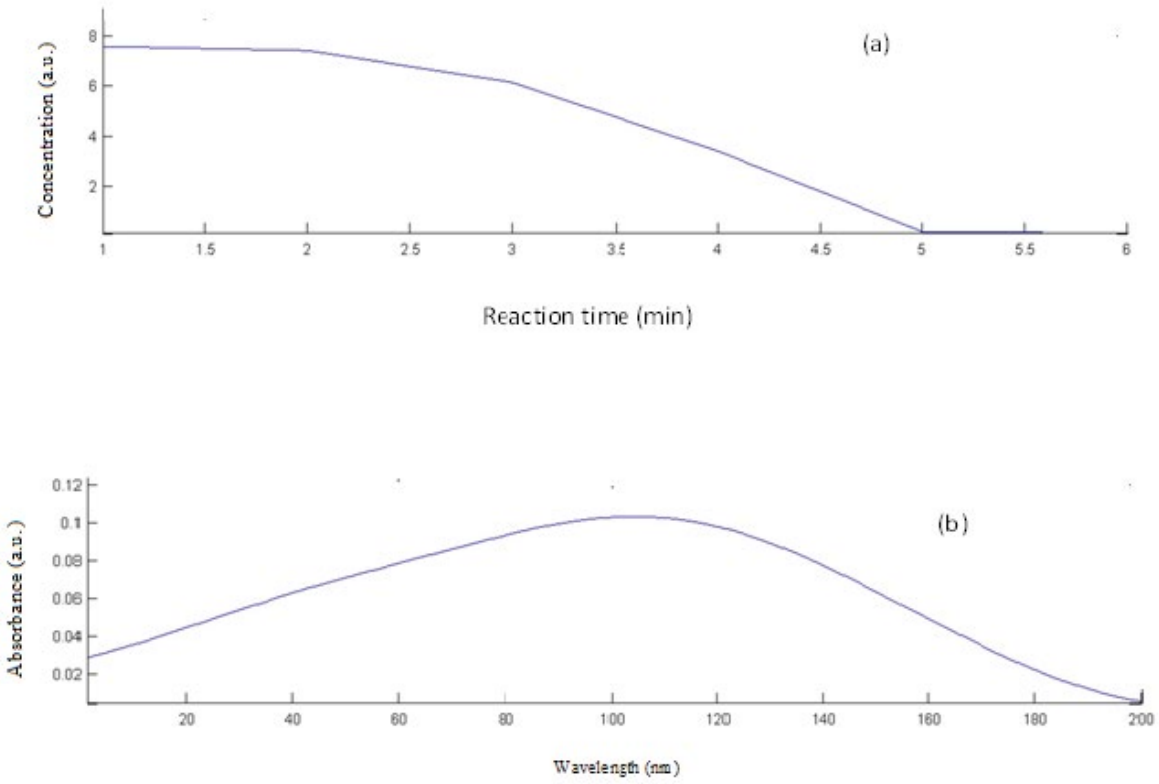

Fig. 7. Data profile of nitrite solution resolved by the MCR-ALS method. (a) Concentration profile and (b) spectral profile.

4. Conclusions

In the present study, the preparation and optimization of chitosan/hydroxyapatite (HAp/CS) nano hybrid as adsorbent for remove of nitrite from suspension has been investigated. The CCD model was used to statistically optimize parameters and evaluate the main effects of the independent variables on the particle size. The HAp/CS as adsorbent hybrid was also characterized by XRD and FTIR spectroscopy to specify its morphology, functionality, and structure.

In order to removal of nitrite ions by the nano hybrid, cross linked chitosan-apatite nano hybrid was performed and process was monitored by UV-Vis spectrophotometry. The UV-Vis spectrum of cross linked chitosan-apatite nano hybrid suspension was recorded every 5 min to obtain and evaluate the equilibrium concentration. Also,

in order to investigate the evolution of adsorption process was investigated by MCR-ALS method.

References

[1] S. Bolisetty, M. Peydayesh, R. Mezzenga, Sustainable technologies for water purification from heavy metals: review and analysis, Chem. Soc. Rev., 48 (2019) 463–487.

[2] S. Ahuja, Advances in Water Purification Techniques, Elsevier Inc., 2019, pp. 1–15.

[3] B.H. Hill, C.M. Elonen, A.T. Herlihy, T.M. Jicha, G. Serenbetz, Microbial ecoenzyme stoichiometry, nutrient limitation, and organic matter decomposition in wetlands of the conterminous United States, Wetlands Ecol. Manage., 26 (2018) 425–439.

[4] S.F. Johnson, Methemoglobinemia: infants at risk, Curr. Probl. Pediatr. Adolesc. Health Care, 49 (2019) 57–67.

[5] J.W. Palko, D.I. Oyarzun, B. Ha, M. Stadermann, J.G. Santiago, Nitrate removal from water using electrostatic regeneration of functionalized adsorbent, Chem. Eng. J., 334 (2018) 1289–1296.

[6] X. Rao, X. Shao, J. Xu, J. Yi, J. Qiao, Q. Li, M. Chien, C. Inoue, Y. Liu, J. Zhang, Efficient nitrate removal from water using selected cathodes and Ti/PbO_2 anode: experimental study and mechanism verification, Sep. Purif. Technol., 216 (2019) 158–165.

[7] P.S. Kumar, P.R. Yaashikaa, S. Ramalingam, Efficient Removal of Nitrate and Phosphate Using Graphene Nanocomposites, Springer International Publishing, 2019.

[8] A. Bhatnagar, E. Kumar, M. Sillanpää, Nitrate removal from water by nano-alumina: characterization and sorption studies, Chem. Eng. J., 163 (2010) 317–323.

[9] F. Ruiz-Beviá, M.J. Fernández-Torres, Effective catalytic removal of nitrates from drinking water: an unresolved problem?, J. Cleaner Prod., 217 (2019) 398–408.

[10] N.R. Kheirabadi, N.S. Tabrizi, P. Sangpour, Removal of nitrate from water by alginate - derived carbon aerogel modified by protonated cross-linked chitosan, J. Polym. Environ., 27 (2019) 1642–1652.

[11] S. Periyasamy, P. Manivasakan, C. Jeyaprabha, S. Meenakshi, N. Viswanathan, Fabrication of nano-graphene oxide hydrotalcite/chitosan biocomposite: an efficient adsorbent for chromium removal from water, Int. J. Biol. Macromol., 132 (2019) 1068–1078.

[12] C. da Silva, A. Prasniewski, M.A. Calegari, V.A. de Lima, T.L.C. Oldoni, Determination of total phenolic compounds and antioxidant activity of ethanolic extracts of propolis using ATR–FT-IR spectroscopy and chemometrics, Food Anal. Methods, 11 (2018) 2013–2021.

[13] F. Rezvani, M. Sarrafzadeh, S. Ebrahimi, H.M. Oh, Nitrate removal from drinking water with a focus on biological methods: a review, Environ. Sci. Pollut. Res., 26 (2017) 1124–1141.

[14] Z. Zhang, Z. Hao, Y. Yang, J. Zhang, Q. Wang, X. Xu, Reductive denitrification kinetics of nitrite by zero-valent iron, Desalination, 257 (2010) 158–162.

[15] N. Öztürk, T.E. Köse, A kinetic study of nitrite adsorption onto sepiolite and powdered activated carbon, Desalination, 223 (2008) 174–179.

[16] G. Crini, Historical review on chitin and chitosan biopolymers, Environ. Chem. Lett., 17 (2019) 1623–1643.

[17] J.K.H. Wong, H.K. Tan, S.Y. Lau, P.-S. Yap, M. Kobina Danquah, Potential and challenges of enzyme incorporated nanotechnology in dye wastewater treatment: a review, J. Environ. Chem. Eng., 7 (2019) 103261.

[18] E. Avcu, F.E. Baştan, H.Z. Abdullah, M.A. Ur Rehman, Y. Yildiran Avcu, A.R. Boccaccini, Electrophoretic deposition of chitosan-based composite coatings for biomedical applications: a review, Prog. Mater. Sci., 103 (2019) 69–108.

[19] M. Rajamani, K. Rajendrakumar, Chitosan-boehmite desiccant composite as a promising adsorbent towards heavy metal removal, J. Environ. Manage., 244 (2019) 257–264.

[20] B. Yu, Q. Huang, Y. Liu, G. Jiang, Fabrication of composite biofibres based on chitosan and fluorinated graphene for adsorption of heavy metal ions in water, J. Text. Inst., 110 (2018) 426–434.

[21] N. Zerbinati, T. Lotti, D. Monticelli, R. Rauso, P. González-Isaza, E. D'Este, A. Calligaro, S. Sommatis, C. Maccario, R. Mocchi, J. Lotti, U. Wollina, G. Tchernev, K. França, In vitro evaluation of the biosafety of hyaluronic acid PEG cross-linked with micromolecules of calcium hydroxyapatite in low concentration, Open Access Maced. J. Med. Sci., 6 (2018) 15–19.

[22] I. Grigoraviciute-Puroniene, A. Zarkov, K. Tsuru, K. Ishikawa, A. Kareiva, A novel synthetic approach for the calcium hydroxyapatite from the food products, J. Sol-Gel Sci. Technol., 91 (2019) 63–71.

[23] M. Ibrahim, M. Labaki, J.M. Giraudon, J.F. Lamonier, Hydroxyapatite, a multifunctional material for air, water and soil pollution control: a review, J. Hazard. Mater., 383 (2020) 121139.

[24] Y. Chen, J. Yu, Q. Ke, Y. Gao, C. Zhang, Y. Guo, Bioinspired fabrication of carbonated hydroxyapatite/chitosan nanohybrid scaffolds loaded with TWS119 for bone regeneration, Chem. Eng. J., 341 (2018) 112–125.

[25] J. Xia, J. Zhang, Y. Zhao, Y. Huang, Y. Xiong, S. Min, Fourier transform infrared spectroscopy and chemometrics for the discrimination of paper relic types, Spectrochim. Acta, Part A, 219 (2019) 8–14.

[26] R.G. Brereton, Pattern recognition in chemometrics, Chemom. Intell. Lab. Syst., 149 (2015) 90–96.

[27] R.G. Brereton, Chemometrics: Data Analysis for the Laboratory and Chemical Plant, Wiley, Bristol, 2003.

[28] J. Jaumot, A. De Juan, R. Tauler, MCR-ALS GUI 2.0: new features and applications, Chemom. Intell. Lab. Syst., 140 (2015) 1–12.

[29] E. García-Robledo, A. Corzo, S. Papaspyrou, A fast and direct spectrophotometric method for the sequential determination of nitrate and nitrite at low concentrations in small volumes, Mar. Chem., 162 (2014) 30–36.

[30] V. Sureshkumar, S.C.J. Kiruba Daniel, K. Ruckmani, M. Sivakumar, Fabrication of chitosan – magnetite nanocomposite strip for chromium removal, Appl. Nanosci., 6 (2015) 277–285.

[31] S.N. Danilchenko, O.V. Kalinkevich, M.V. Pogorelov, A.N. Kalinkevich, A.M. Sklyar, T.G. Kalinichenko, V.Y. Ilyashenk, V.V. Starikov, V.I. Bumeyster, V.Z. Sikora, L.F. Sukhodub, A.G. Mamalis, S.N. Lavrynenko, J.J. Ramsden, Chitosan-hydroxyapatite composite biomaterials made by one step co-precipitation method: preparation, characterization and in vivo tests, J. Biol. Phys. Chem., 9 (2009) 119–126.

[32] P. Karthikeyan, H.A. Thagira Banu, S. Meenakshi, Removal of phosphate and nitrate ions from aqueous solution using La^{3+} incorporated chitosan biopolymeric matrix membrane, Int. J. Biol. Macromol., 124 (2019) 492–504.

[33] S. Mondal, A. Dey, U. Pal, Low temperature wet-chemical synthesis of spherical hydroxyapatite nanoparticles and their *in situ* cytotoxicity study, Adv. Nano Res., 4 (2016) 295–307.

[34] M.R. Alcaraz, A. Aguirre, H.C. Goicoechea, M.J. Culzoni, S.E. Collins, Resolution of intermediate surface species by combining modulated infrared spectroscopy and chemometrics, Anal. Chim. Acta, 1049 (2019) 38–46.

[35] M. Babaee Rouchi, M. Khanmohammadi, A. Bagheri Garmarudi, M. De La Guardia, Application of infrared spectroscopy as process analytics technology (PAT) approach in biodiesel production process utilizing multivariate curve resolution alternative least square (MCR-ALS), Spectrochim. Acta, Part A, 213 (2019) 347–353.